Hindawi
Journal of Sensors
Volume 2021, Article ID 1745383, 8 pages
https://doi.org/10.1155/2021/1745383

Research Article

A State-Domain Robust Chi-Square Test Method for GNSS/INS Integrated Navigation

Zhangjun Yu, Qiuzhao Zhang, Ke Yu, and Nanshan Zheng

School of Environment Science and Spatial Informatics, China University of Mining and Technology, Xuzhou 221116, China

Correspondence should be addressed to Qiuzhao Zhang; qiuzhao.zhang@cumt.edu.cn

Received 3 June 2021; Revised 27 August 2021; Accepted 11 September 2021; Published 7 October 2021

Academic Editor: Aijun Yin

Aiming at abrupt faults in GNSS/INS integrated systems in complex environments, classical fault detection algorithms are mostly developed from the measurement domain. A robust chi-square test method based on the state domain is proposed in this paper. The fault detection statistic is built based on the difference between the prior state estimation and the posterior state estimation in Kalman filtering. To improve the calculation stability, singular value decomposition (SVD) is used to factor the covariance matrix of the difference. The relevant formulas of the proposed method were theoretically derived, and the relationship between the proposed method and the existing innovation chi-square test method was revealed. The proposed method was compared with state-of-the-art chi-square test methods and verified by GNSS/INS integrated navigation experiments using simulation data and real data. The experimental results show that the proposed method (a) directly works in the state domain, (b) does not require the known real system state, (c) has computational efficiency and good robustness, and (d) accurately detects abrupt faults.

1. Introduction

To take full advantage of each individual navigation system and overcome their shortcomings, integrated navigation systems based on Global Navigation Satellite System (GNSS) and Inertial Navigation System (INS) are widely used in positioning and attitude determination applications [1]. Kalman filtering plays an important role in the integration of GNSS and INS data. A basic assumption for applying standard Kalman filtering is that both the dynamic model and the stochastic information provided to the filter are accurate [2]. If this assumption is not valid or there are many outliers, the Kalman filter may result in poor performance such as abrupt faults in the filtering result [3, 4]. Therefore, it is necessary to carry out real-time fault detection to ensure the reliability and precision of the integrated navigation system [5, 6].

In the field of integrated navigation fault detection, chi-square test methods are the classical methods and are widely used because they can detect the faults caused by outliers in the measurements and inaccurate dynamic models or random information of the Kalman filter. The methods determine the fault detection threshold by the probability of a false alarm (FA) specified in the integrated navigation system, so they do not require any user interaction. The methods can be principally divided into two groups [7–9]:

(i) *State chi-square test methods*: detect faults through the state estimate error. A state chi-square test method, which directly detects faults based on the difference between the true state and the posterior state estimate, was proposed in [10]; however, it requires knowledge of the true state and is thus suitable for simulation-based fault detection, not for real-time fault detection. The state chi-square test method, which is based on a state propagator and detects faults based on the difference between the estimate of the state propagator and the posterior state estimate, is affected by the initial system value error, the system noise, and the modelling error as

it works, and the state propagator value will deviate increasingly from the true value because there is no measurement update [11]. The double-state chi-square test method uses two state propagators that work alternately and correct each other, which can avoid the problem of no measurement update, but the fault detection rate and calculation efficiency will decrease over time [12–17]

(ii) *Innovation chi-square test methods*: detect faults through the innovation (i.e., the measurement prediction error). The innovation chi-square test method, which indirectly detects faults based on the difference between the true measurement and the predictive measurement, can detect abrupt faults in time with a small amount of calculation [18–22]. In [23], the Federal Kalman filter based on the innovation chi-square test method is used in suborbital vehicles, and the results show that the proposed method can quickly correct the errors caused by GPS abrupt faults within 1 s. However, this method provides a direct assessment of the measurement prediction error but only an indirect assessment of the filtering state estimate error. In fact, accurate and consistent measurement predictions do not necessarily result in accurate and consistent state estimates [24]

The goal of the paper is to propose a state-domain robust fault detection method addressing the aforementioned limitations of the state-of-the-art tests, i.e., to design a method that (a) directly works in the state domain, (b) does not require the known real system state, (c) has computational efficiency (i.e., detect faults without state propagators) and good robustness, and (d) accurately detects the abrupt fault.

The remainder of this paper is organized as follows. Section 2 lists the formulas of the dynamic and observation equations of the GNSS/INS system. In Section 3, the innovation chi-square test method is reviewed and analysed. The state-domain robust fault detection method is described in Section 4. The experimental description and analysis are given in Section 5. Finally, the paper is concluded in Section 6.

2. The Dynamic and Observation Equations of the GNSS/INS System

A loosely coupled GNSS/INS system is adopted. The state vectors are composed of the position and velocity error in an earth-centered and earth-fixed frame (ECEF frame, e frame), the attitude error is described between the computer e frame and the platform e' frame, and the gyro and accelerometer drift error is in the body frame (b frame), which can be expressed as [25–27]

$$\mathbf{x}_k = \left[\Delta\mathbf{R}^e \Delta\mathbf{V}^e \boldsymbol{\varphi}^e \nabla^b \boldsymbol{\varepsilon}^b\right]^T. \tag{1}$$

The nonlinear differential error model of a low-cost INS is as follows:

$$\begin{cases} \Delta\dot{\mathbf{R}}^e = \Delta\mathbf{V}^e, \\ \Delta\dot{\mathbf{V}}^e = \left(\mathbf{I}_{3\times3} - \mathbf{C}_{e'}^{e}\right)\mathbf{f}^{e'} + \mathbf{C}_b^{e'}\nabla^b - 2\boldsymbol{\Omega}_{ie}^e\Delta\mathbf{V}^e, \\ \dot{\boldsymbol{\varphi}}^e = \left(\mathbf{I}_{3\times3} - \mathbf{C}_e^{e'}\right)\boldsymbol{\omega}_{ie}^e - \mathbf{C}_b^{e'}\boldsymbol{\varepsilon}^b, \\ \dot{\nabla}^b = 0, \\ \dot{\boldsymbol{\varepsilon}}^b = 0, \end{cases} \tag{2}$$

where $\Delta\mathbf{R}^e$ and $\Delta\mathbf{V}^e$ are the position and velocity error in the e frame, respectively; $\dot{\boldsymbol{\varphi}}^e$ is the attitude error between the computer e frame and the platform e' frame; $\mathbf{I}_{3\times3}$ is a 3×3 unit matrix; $\mathbf{C}_{e'}^{e}$ is the rotation matrix between the computer e frame and the platform e' frame; $\mathbf{C}_b^{e'}$ is the rotation matrix between the body frame and the platform e' frame; $\boldsymbol{\Omega}_{ie}^e$ is the skew symmetric matrix of the earth rotation rate $\boldsymbol{\omega}_{ie}^e$; and $\boldsymbol{\varepsilon}^b$ and ∇^b are gyro and accelerometer drift errors in the body frame, respectively.

The dynamic model of a loosely coupled GNSS/INS system can be expressed as follows:

$$\mathbf{x}_{k+1} = \mathbf{f}_k(\mathbf{x}_k) + \mathbf{w}_k, \tag{3}$$

where the vector $\mathbf{x}_k$ represents the state of the system, $\mathbf{f}_k$ is the system function, and $\mathbf{w}_k$ is the process noise vector, which is commonly assumed to be zero-mean Gaussian white noise with covariance matrix $\mathbf{Q}_k$.

Generally, the measurement model can be expressed as

$$\mathbf{z}_k = \begin{bmatrix} \widehat{\mathbf{R}}_{\mathrm{INS}}^e - \widehat{\mathbf{R}}_{\mathrm{GPS}}^e \\ \widehat{\mathbf{V}}_{\mathrm{INS}}^e - \widehat{\mathbf{V}}_{\mathrm{GPS}}^e \end{bmatrix} = \mathbf{h}_k(\mathbf{x}_k) + \mathbf{v}_k, \tag{4}$$

where the vector $\mathbf{z}_k$ represents the measurement, $\widehat{\mathbf{R}}_{\mathrm{INS}}^e$ and $\widehat{\mathbf{V}}_{\mathrm{INS}}^e$ are the INS-computed position and velocity vectors in the e frame, $\widehat{\mathbf{R}}_{\mathrm{GPS}}^e$ and $\widehat{\mathbf{V}}_{\mathrm{GPS}}^e$ are the GNSS vector outputs, $\mathbf{h}_k$ is the measurement function, and $\mathbf{v}_k$ is the measurement noise vector, which is commonly assumed to be zero-mean Gaussian white noise with covariance matrix $\mathbf{R}_k$.

3. Problem Formulation

Fault detection is a vital and safety-related task for integrated navigation systems. In this section, the Kalman filter for GNSS/INS integrated navigation is formulated and the innovation chi-square test method, which is a popular and widely discussed test used for several decades, is introduced and analysed.

3.1. Kalman Filter for GNSS/INS Integrated Navigation. The methods purposely designed for abrupt fault detection in the integrated navigation system are based on the Gaussian assumption and the statistical hypothesis testing. Therefore,

let a state variable $\mathbf{x}$ with a known prior Gaussian probability density function (PDF)

$$p(\mathbf{x}) = \mathcal{N}\left\{\mathbf{x}; \hat{\mathbf{x}}', \mathbf{P}'_{xx}\right\} \tag{5}$$

be considered, where the notation $\mathcal{N}\{\mathbf{x}; \hat{\mathbf{x}}', \mathbf{P}'_{xx}\}$ stands for the normal distribution with the mean $\hat{\mathbf{x}}' = E[\mathbf{x}]$ and the covariance matrix $\mathbf{P}'_{xx} = \text{cov}[\mathbf{x}]$; meanwhile, the time update and measurement update of the Kalman filter for GNSS/INS integrated navigation can be expressed as follows:

$$\hat{\mathbf{x}}_k = \hat{\mathbf{x}}'_k + \mathbf{K}_k\left(\mathbf{z}_k - \hat{\mathbf{z}}'_k\right), \tag{6}$$

$$\mathbf{K}_k = \mathbf{P}'_{xz,k}\left(\mathbf{P}'_{zz,k}\right)^{-1}, \tag{7}$$

$$\mathbf{P}_{xx,k} = \mathbf{P}'_{xx,k} - \mathbf{K}_k\mathbf{P}'_{zz,k}(\mathbf{K}_k)^T, \tag{8}$$

$$\hat{\mathbf{x}}'_{k+1} \approx \int \mathbf{f}_k(\mathbf{x}_k)\mathcal{N}\left\{\mathbf{x}_k; \hat{\mathbf{x}}_k, \mathbf{P}_{xx,k}\right\}d\mathbf{x}_k, \tag{9}$$

$$\mathbf{P}'_{xx,k+1} \approx \int\left(\mathbf{f}_k(\mathbf{x}_k) - \widehat{\mathbf{x}'}_{k+1}\right)\left(\mathbf{f}_k(\mathbf{x}_k) - \widehat{\mathbf{x}'}_{k+1}\right)\mathcal{N} \cdot \left\{\mathbf{x}_k; \hat{\mathbf{x}}_k, \mathbf{P}_{xx,k}\right\}d\mathbf{x}_k + \mathbf{Q}_k, \tag{10}$$

$$\hat{\mathbf{z}}'_k \approx \int \mathbf{h}_k(\mathbf{x}_k)\mathcal{N}\left\{\mathbf{x}_k; \hat{\mathbf{x}}'_k, \mathbf{P}'_{xx,k}\right\}d\mathbf{x}_k, \tag{11}$$

$$\mathbf{P}'_{zz,k} \approx \int\left(\mathbf{h}_k(\mathbf{x}_k) - \hat{\mathbf{z}}'_k\right)\left(\mathbf{h}_k(\mathbf{x}_k) - \hat{\mathbf{z}}'_k\right)\mathcal{N}\left\{\mathbf{x}_k; \hat{\mathbf{x}}'_k, \mathbf{P}'_{xx,k}\right\}d\mathbf{x}_k + \mathbf{R}_k, \tag{12}$$

$$\mathbf{P}'_{xz,k} \approx \int\left(\mathbf{x}_k - \widehat{\mathbf{x}'}_k\right)\left(\mathbf{h}_k(\mathbf{x}_k) - \hat{\mathbf{z}}'_k\right)\mathcal{N}\left\{\mathbf{x}_k; \hat{\mathbf{x}}'_k, \mathbf{P}'_{xx,k}\right\}d\mathbf{x}_k, \tag{13}$$

where $\hat{\mathbf{x}}'_k$ is the prior state estimate, $\mathbf{P}'_{xx,k}$ is the covariance matrix of $\hat{\mathbf{x}}'_k$, $\mathbf{K}_k$ is the gain matrix, $\hat{\mathbf{x}}_k$ is the posterior state estimate, $\mathbf{P}_{xx,k}$ is the covariance matrix of $\hat{\mathbf{x}}_k$, $\hat{\mathbf{z}}'_k$ is the predictive measurement, $\mathbf{P}'_{zz,k}$ is the covariance matrix of $\hat{\mathbf{z}}'_k$, and $\mathbf{P}'_{xz,k}$ is the "crosscovariance" matrix of joint $\hat{\mathbf{x}}'_k$ and $\hat{\mathbf{z}}'_k$.

3.2. The Innovation Chi-Square Test Method. In principle, the detection of the abrupt faults can be formulated using statistical hypothesis testing. The null hypothesis H_0: assuming no fault, i.e., assuming $\hat{\mathbf{x}}_k$ and $\mathbf{P}_{xx,k}$, is accurate enough, which is tested against the alternative hypothesis H_1: assuming there is a fault.

The innovation chi-square test method that detects abrupt faults by predictive measurement $\hat{\mathbf{z}}'_k$ and measurement $\mathbf{z}_k$ is described as follows:

Step 1. Define a required (or allowed) probability of false alert P_{FA}.

Step 2. Compute statistic

$$\mathcal{Z}_k = (\mathbf{e}_k)^T\left(\mathbf{P}'_{zz,k}\right)^{-1}\mathbf{e}_k, \quad \mathcal{Z}_k \sim p(\mathcal{Z}_k). \tag{14}$$

If the null hypothesis H_0 is valid, then the PDF $p(\mathcal{Z}_k)$ is (approximately) a chi-squared distribution with n_z degrees of freedom (DOF), where $\mathbf{e}_k = \mathbf{z}_k - \hat{\mathbf{z}}'_k$ and n_z is the dimension of the measurement domain.

Step 3. Compute the corresponding P_{FA} quantile

$$q^{\mathcal{Z}}_{\text{FA},k} = \inf\{\mathcal{Z}_k \in : (1 - P_{\text{FA}}) \le F(\mathcal{Z}_k)\}, \tag{15}$$

where $F(\mathcal{Z}_k)$ is the cumulative distribution function with respect to $p(\mathcal{Z}_k)$ and the operator inf stands for the infimum. The quantile $q^{\mathcal{Z}}_{\text{FA},k}$ is further denoted as the fault detection threshold.

Step 4. Compare the statistic $\mathcal{Z}_k$ (14) with the threshold $q^{\mathcal{Z}}_{\text{FA},k}$ (15). If $\mathcal{Z}_k \le q^{\mathcal{Z}}_{\text{FA},k}$, then it is considered to be no fault. Otherwise, it would be considered to have a fault.

However, this method provides a direct assessment of the measurement prediction error $\mathbf{e}_k$ but just an indirect assessment of the filtering state estimate error. In fact, accurate and consistent measurement predictions do not necessarily result in accurate and consistent state estimates. The measurement domain test assumes the Gaussian of the measurement prediction PDF and therefore cannot consider the error in computation of the "crosscovariance" matrix $\mathbf{P}'_{xz,k}$ [24].

4. The State-Domain Robust Chi-Square Test Method

In this section, the state-domain robust chi-square test method is proposed.

4.1. Derivation. The proposed test is based on a statistical analysis of the difference between prior and posterior state estimates defined as

$$\mathbf{d}_k = \hat{\mathbf{x}}_k - \hat{\mathbf{x}}'_k. \tag{16}$$

Its statistical properties are summarized in the following theorem.

Theorem 1. *Under valid hypothesis H_0, the difference $\mathbf{d}_k$ is a random variable with*

$$\hat{\mathbf{d}}_k = E[\mathbf{d}_k] = 0_{n_x}, \tag{17}$$

$$\mathbf{P}_{dd,k} = \mathbf{P}'_{xx,k} - \mathbf{P}_{xx,k} = \mathbf{K}_k\mathbf{P}'_{zz,k}(\mathbf{K}_k)^T, \tag{18}$$

where n_x is the dimension of the state domain.

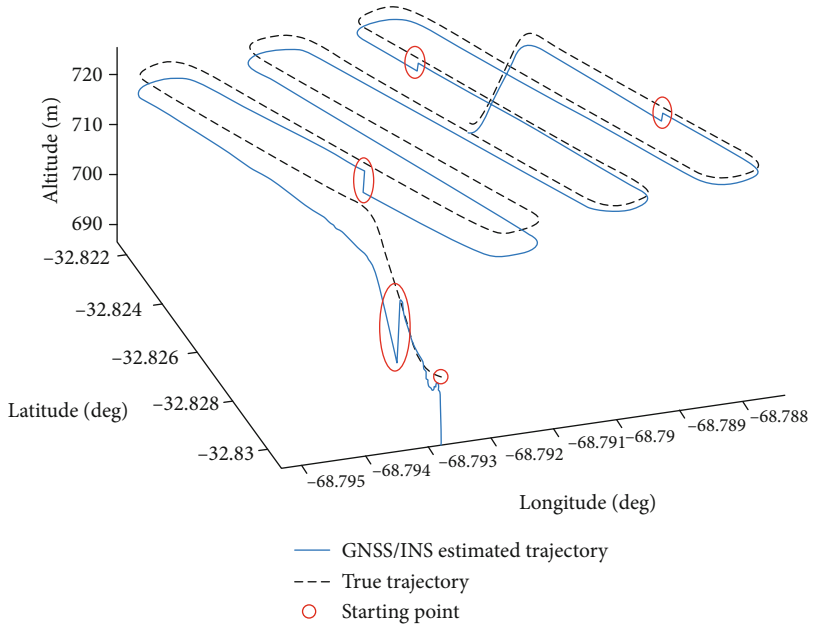

Figure 1: The true trajectory and the GNSS/INS estimated trajectory.

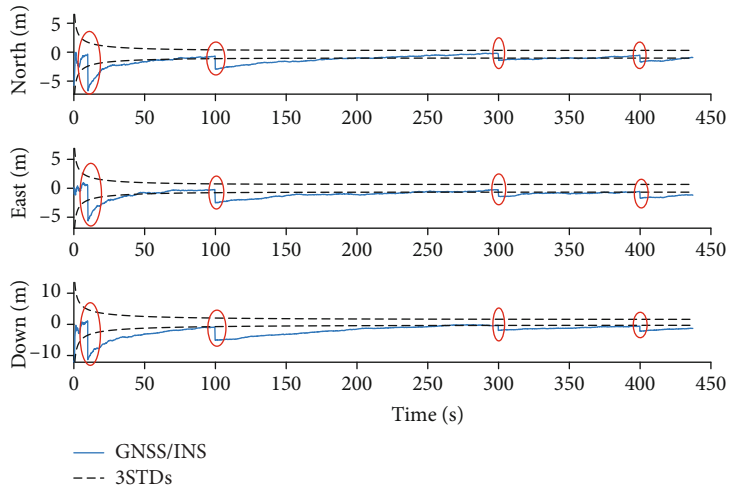

Figure 2: The position error using the simulation data and the confidence region defined by ±3STDs.

Proof. The proof of (17): both the prior and posterior mean estimates are unbiased, i.e., $\hat{\mathbf{x}}_k' = \hat{\mathbf{x}}_k = E[\mathbf{x}_k]$. The proof of (18): the difference $\mathbf{d}_k$ (16) can be written as

$$\mathbf{d}_k = \mathbf{x}_k - \hat{\mathbf{x}}_k' - (\mathbf{x}_k - \hat{\mathbf{x}}_k) = \tilde{\mathbf{x}}_k' - \tilde{\mathbf{x}}_k, \tag{19}$$

where $\tilde{\mathbf{x}}_k'$ is the prior state estimate error and $\tilde{\mathbf{x}}_k$ is the posterior state estimate error.

$$\mathbf{P}_{dd,k} = E\left[\mathbf{d}_k \mathbf{d}_k^T\right] = \mathbf{P}'_{xx,k} + \mathbf{P}_{xx,k} - \mathbf{M}_{x'x,k} - \mathbf{M}_{xx',k}, \tag{20}$$

where the (cross-)second-order moment of the posterior and prior state estimate error is defined as $\mathbf{M}_{x'x,k} = E[\tilde{\mathbf{x}}_k' \tilde{\mathbf{x}}_k^T]$, and $\mathbf{M}_{x'x,k} = (\mathbf{M}_{xx',k})^T$.

$$\begin{aligned} \mathbf{M}_{x'x,k} &= E\left[\left(\mathbf{x}_k - \hat{\mathbf{x}}_k'\right)\left(\mathbf{x}_k - \hat{\mathbf{x}}_k' - \mathbf{K}_k\left(\mathbf{z}_k - \hat{\mathbf{z}}_k'\right)\right)^T\right] \\ &= \mathbf{P}'_{xx,k} - \mathbf{P}'_{xz,k}(\mathbf{K}_k)^T \\ &= \mathbf{P}_{xx,k}. \end{aligned} \tag{21}$$

Then, by substituting (21) into (20), the expression for (18) is obtained. □

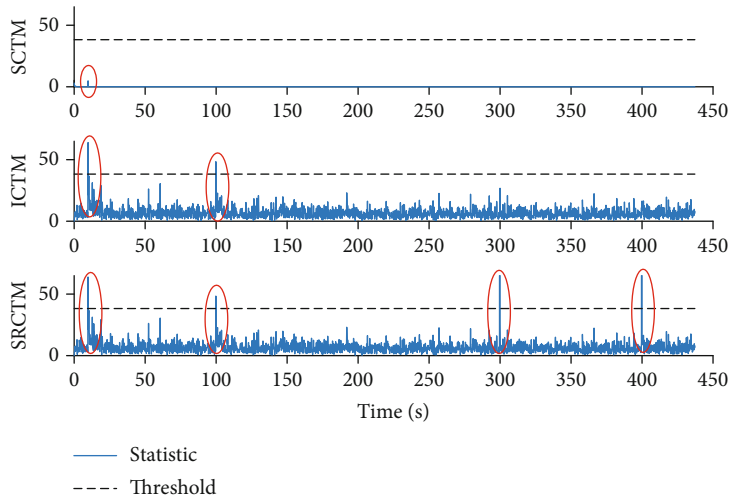

Figure 3: Statistics of the different methods using the simulation data.

4.2. Algorithm. The state-domain robust chi-square test method that detects abrupt faults by the difference $\mathbf{d}_k$ is described as follows:

Step 1. Define a required (or allowed) probability of false alert P_{FA}.

Step 2. Compute statistic

$$\mathscr{C}_k = (\mathbf{d}_k)^T (\mathbf{P}_{dd,k})^{-1} \mathbf{d}_k, \quad \mathscr{C}_k \sim p(\mathscr{C}_k). \tag{22}$$

If the null hypothesis H_0 is valid, then the PDF $p(\mathscr{C}_k)$ is (approximately) a chi-squared distribution with n_x DOF. To improve the calculation stability, singular value decomposition (SVD) is used to factor $\mathbf{P}_{dd,k}$.

Step 3. Compute the corresponding P_{FA} quantile

$$q^{\mathscr{C}}_{\mathrm{FA},k} = \inf \{\mathscr{C}_k \in : (1 - P_{\mathrm{FA}}) \le F(\mathscr{C}_k)\}, \tag{23}$$

where $F(\mathscr{C}_k)$ is the cumulative distribution function with respect to $p(\mathscr{C}_k)$.

Step 4. Compare the statistic $\mathscr{C}_k$ (22) with the threshold $q^{\mathscr{C}}_{\mathrm{FA},k}$ (23). If $\mathscr{C}_k \le q^{\mathscr{C}}_{\mathrm{FA},k}$, then it is considered to be no fault. Otherwise, it would be considered to have a fault.

4.3. Relationship between the Proposed Method and the Innovation Chi-Square Test Method. The innovation chi-square test method can be seen as a special case of the proposed method under the consideration of certain simplifications.

With respect to (6) and (8), the difference $\mathbf{d}_k$ and $\mathbf{P}_{dd,k}$ can be written as

$$\begin{aligned} \mathbf{d}_k &= \mathbf{K}_k \mathbf{e}_k, \\ \mathbf{P}_{dd,k} &= \mathbf{K}_k \mathbf{P}'_{zz,k} (\mathbf{K}_k)^T. \end{aligned} \tag{24}$$

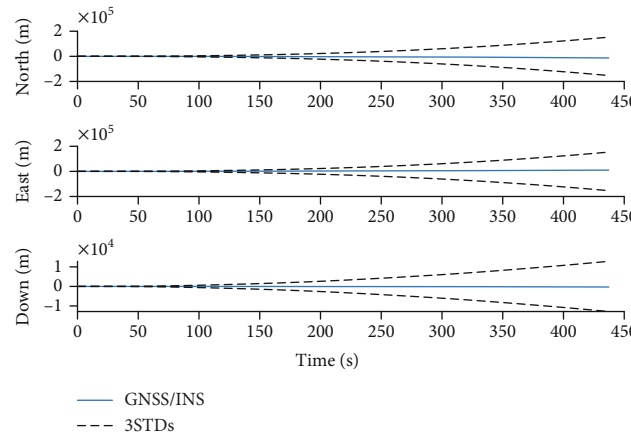

Figure 4: The position error using the simulation data and the confidence region of the state propagator defined by 3STDs.

Assuming $n_x = n_z$, $\mathbf{K}_k$ is invertible, and faults caused by the outliers in the measurements and inaccurate dynamic models or random information of the Kalman filter, the statistic $\mathscr{C}_k$ (22) can be further treated as

$$\begin{aligned} \mathscr{C}_k &= (\mathbf{e}_k)^T (\mathbf{K}_k)^T \left(\mathbf{K}_k \mathbf{P}'_{zz,k} (\mathbf{K}_k)^T \right)^{-1} \mathbf{K}_k \mathbf{e}_k \\ &= (\mathbf{e}_k)^T \left(\mathbf{P}'_{zz,k} \right)^{-1} \mathbf{e}_k \\ &= \mathscr{Z}_k. \end{aligned} \tag{25}$$

In this case, the proposed method is equivalent to the innovation chi-square test method.

5. Experiment Description

In this section, the proposed method, called the state-domain robust chi-square test method (SRCTM), is compared with the innovation chi-square test method (ICTM) and the state chi-square test method (SCTM) and verified

Figure 5: The University of Nottingham test vehicle.

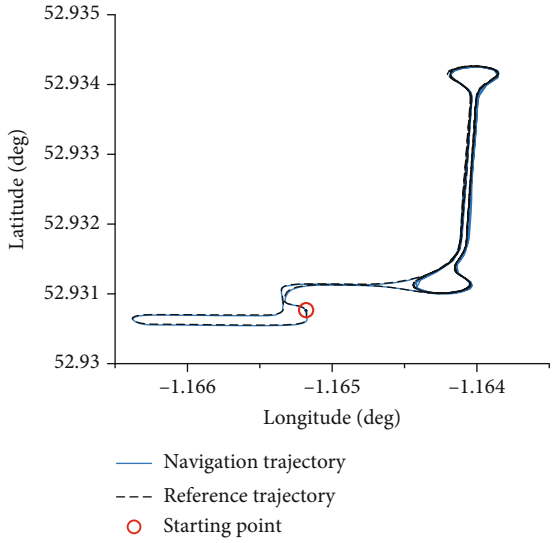

Figure 6: The test trajectory.

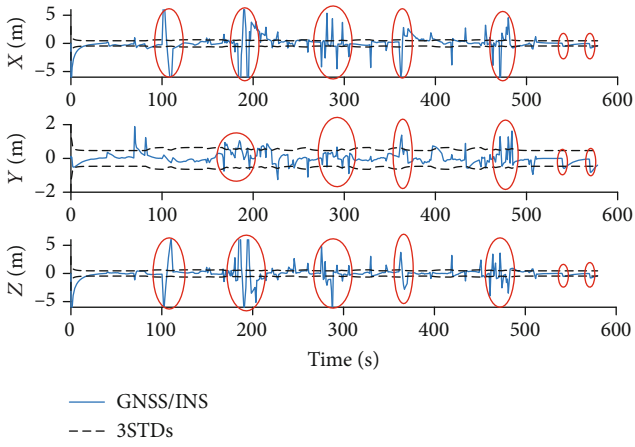

Figure 7: The position error using the real data and the confidence region defined by ±3STDs.

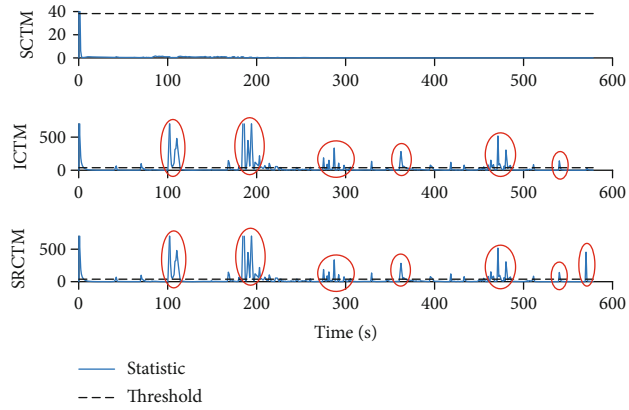

Figure 8: Statistics of the different methods using the real data.

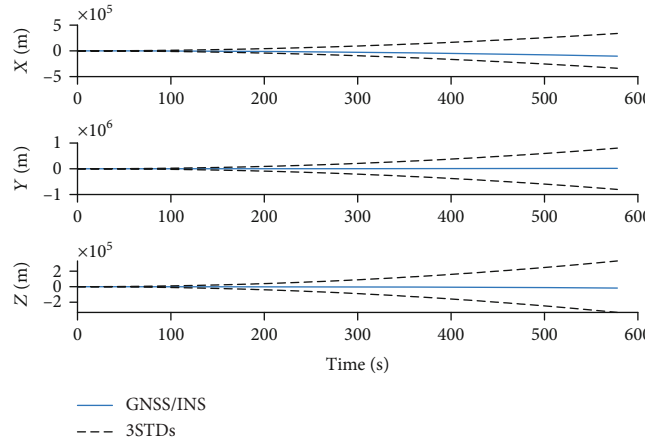

Figure 9: The position error using the real data and the confidence region of the state propagator defined by 3STDs.

by GNSS/INS integrated navigation experiments using simulation data and real data. To objectively compare the efficiency of the different methods, the probability of false alerts P_{FA} is set as 10^{-6} and $n_x = n_z = 6$. Meanwhile, the same hardware and software are adopted. The hardware is a PC with a Core i5-10500 CPU and 16 GB RAM. The R2019b version of MATLAB software running on a Windows 10 system is used to design the different algorithms.

5.1. GNSS/INS Integrated Navigation Experiment Using the Simulation Data. The GNSS/INS integrated navigation experiment using simulation data utilized a simulation framework for low-cost integrated navigation systems called NaveGo, which simulates measurements from inertial sensors and a GNSS receiver. It is found that the absolute differences between real and simulated systems are under 23

centimeters for 2D position and under 10 centimeters for vertical position [28].

To verify the effectiveness of the SRCTM and compare it with the ICTM and the RCTM, two abrupt faults based on the standard deviation (STD) as 9STDs were added in the dynamic model (3) artificially at 10 s and 100 s, and two abrupt faults based on the STD as 5STDs were added in the posterior state estimate (6) artificially at 300 s and 400 s. Figure 1 shows the true trajectory and the estimated trajectory, which contains the abrupt faults.

Figure 2 contains the position error of the GNSS/INS and confidence region based on the STD as ±3STDs, and the error exceeds 3STDs at the time when the abrupt fault is added.

Figure 3 shows the statistics of the different methods, and both the ICTM and the SRCTM are very sensitive to abrupt faults in the dynamic model. Only the SRCTM can detect faults in the posterior state estimate (because the SRCTM is based on the difference between the prior and posterior state estimates). In addition, the SRTM can hardly detect faults, and the statistics change only in the initial period, because the state propagator value will deviate increasingly from the true value without measurement update. Note that the SRTM is clearly more time-consuming than the ICTM and the SRCTM because of the extra state propagator. In Figure 4, the position error using the simulation data and the confidence region of the state propagator defined by 3STDs are provided.

5.2. GNSS/INS Integrated Navigation Experiment Using the Real Data. The GNSS/INS integrated navigation experiment using real data was carried out at the University of Nottingham, UK, in November 2013. A GNSS antenna, a GNSS receiver, and a SPAN-LCI IMU were mounted in a van, and data were logged from the receiver's serial ports to a laptop for storage and processing. The vector between the IMU center and GNSS antenna was accurately surveyed using a total station and was considered accurate within 1 cm. A base station was set up on the roof of the Nottingham Geospatial Building to provide DGPS and RTK corrections. The update rate of INS is 200 Hz, and that of the GNSS is 1 Hz. The average baseline length was less than 3 km for the test. When driving on the roads of the University of Nottingham, the test vehicle performed accelerations and braking at an average speed of at least 20 km/h. Figure 5 is a photograph of the van, and Figure 6 is the test trajectory. The high accuracy real-time output results of the SPAN system are used as the reference value, and the double-difference code GNSS position and velocity results are used as the input measurements.

To verify the effectiveness of the SRCTM and compare it with the SCTM and the ICTM, an abrupt fault based on the STD as 5STDs was artificially added in the measurement model (4) at 540 s, and an abrupt fault based on the STD as 5STDs was added in the posterior state estimate (6) artificially at 570 s. In addition, the results contain some outliers due to the vehicle passing over a speed bump or the data was lost.

Figure 7 contains the position error of the GNSS/INS using real data and the confidence region given by ±3STDs, and the error exceeds 3STDs at the time when the abrupt fault is added or there are many outliers.

Figure 8 shows the statistics of the different methods using the real data, and it can be seen that both the ICTM and the SRCTM are very sensitive to abrupt faults in the measurement model. Only the SRCTM can detect the fault in the posterior state estimate (because the SRCTM is based on the difference between the prior and posterior state estimates). As in Section 5.1, the SRTM can hardly detect the faults, and the statistics change only in the initial period because the state propagator value will deviate increasingly from the true value without measurement update. In Figure 9, the position error using the real data and the confidence region of the state propagator defined by 3STDs are provided.

6. Conclusion

This paper focuses on detecting abrupt faults in integrated navigation systems. A state-domain robust chi-square test method was proposed. Compared to the state-of-the-art method, the proposed method (a) directly works in the state domain, (b) does not require the known real system state, (c) has computational efficiency and good robustness, and (d) can accurately detect abrupt faults. The performance and properties of the proposed method are illustrated in the theoretical derivation and experimental description.

Data Availability

The data that support the findings of this study are available from the corresponding author upon reasonable request.

Conflicts of Interest

The authors declare no conflict of interest.

Acknowledgments

The authors would like to thank Yang Gao and Scott Stephenson from the University of Nottingham for their help in collecting the testing data in Nottingham. This work was supported by the National Key R&D Program of China (2017YFE0119600) and Agentúra na Podporu Výskumu a Vývoja (APVV) (SK-CN-RD-18-0015).

References

[1] D. A. Grejner-Brzezinska, R. Da, and C. Toth, "GPS error modeling and OTF ambiguity resolution for high-accuracy GPS/INS integrated system," *Journal of Geodesy*, vol. 72, no. 11, pp. 626–638, 1998.

[2] C. Hide, T. Moore, and M. Smith, "Adaptive Kalman filtering for low-cost INS/GPS," *Journal of Navigation*, vol. 56, no. 1, pp. 143–152, 2003.

[3] Y. R. Geng and J. L. Wang, "Adaptive estimation of multiple fading factors in Kalman filter for navigation applications," *GPS Solutions*, vol. 12, no. 4, pp. 273–279, 2008.

[4] J. Wang, C. Liu, J. X. Gao, and C. H. Xu, "GNSS/INS tightly coupled navigation model based on robust EKF," *Geomatics and Information Science of Wuhan University*, vol. 36, no. 5, pp. 596–600, 2011.

[5] T. S. Bruggemann, D. G. Greer, and R. A. Walker, "GPS fault detection with IMU and aircraft dynamics," *IEEE Transactions on Aerospace and Electronic Systems*, vol. 47, no. 1, pp. 305–316, 2011.

[6] L. Yi-ting, X. Xiao-su, L. Xi-xiang et al., "A fast gradual fault detection method for underwater integrated navigation systems," *Journal of Navigation*, vol. 69, no. 1, pp. 93–112, 2016.

[7] M. Joerger and B. Pervan, "Kalman filter-based integrity monitoring against sensor faults," *Journal of Guidance, Control, and Dynamics*, vol. 36, no. 2, pp. 349–361, 2013.

[8] B. Brumback and M. Srinath, "A chi-square test for fault-detection in Kalman filters," *IEEE Transactions on Automatic Control*, vol. 32, no. 6, pp. 552–554, 1987.

[9] X. Zhao, S. C. Wang, J. S. Zhang, Z. L. Fan, and H. B. Min, "Real-time fault detection method based on belief rule base for aircraft navigation system," *Chinese Journal of Aeronautics*, vol. 26, no. 3, pp. 717–729, 2013.

[10] Y. Bar-Shalom, T. Kirubarajan, and X. R. Li, *Estimation with Applications to Tracking and Navigation*, Wiley, 2001.

[11] R. Da and C.-F. Lin, "Sensitivity Analysis of the State Chi-Square Test," *IFAC Proceedings*, vol. 29, no. 1, pp. 6596–6601, 1996.

[12] R. Da, "Failure detection of dynamical systems with the state chi-square test," *Journal of Guidance, Control, and Dynamics*, vol. 17, no. 2, pp. 271–277, 1994.

[13] R. Han, H. L. Qin, C. Li, and J. Tian, "A two-stage fault detection structure for JIDS/SINS/GPS integrated navigation system," *Avionics Technology*, vol. 39, no. 3, pp. 43–49, 2008.

[14] H. Q. Zhang, L. I. Dong-Xing, and G. Q. Zhang, "Application of hybrid chi-square test method in fault detection of integrated navigation system," *Journal of Chinese Inertial Technology*, vol. 24, pp. 696–700, 2016.

[15] J. X. Xu, Z. Xiong, J. Y. Liu, and R. Wang, "A dynamic vector-formed information sharing algorithm based on two-state chi square detection in an adaptive federated filter," *Journal of Navigation*, vol. 72, no. 1, pp. 101–120, 2019.

[16] F. Zhang, Y. Wang, and Y. B. Gao, "A novel method of fault detection and identification in a tightly coupled, INS/GNSS-integrated system," *Sensors*, vol. 21, no. 9, p. 2922, 2021.

[17] Z. K. Li, Z. Liu, and L. Zhao, "Improved robust Kalman filter for state model errors in GNSS-PPP/MEMS-IMU double state integrated navigation," *Advances in Space Research*, vol. 67, no. 10, pp. 3156–3168, 2021.

[18] Y. X. Zhu, X. H. Cheng, and L. Wang, "A novel fault detection method for an integrated navigation system using Gaussian process regression," *Journal of Navigation*, vol. 69, no. 4, pp. 905–919, 2016.

[19] C. Yang, J. Guo, L. Zhang, Q. W. Chen, and S. O. Automation, "Fuzzy adaptive unscented Kalman filter integrated navigation algorithm using chi-square test," *Control and Decision*, vol. 33, no. 1, pp. 81–87, 2018.

[20] G. L. Gao, S. S. Gao, G. Y. Hong, X. Peng, and T. Yu, "A robust INS/SRS/CNS integrated navigation system with the chi-square test-based robust Kalman filter," *Sensors*, vol. 20, no. 20, p. 5909, 2020.

[21] Y. T. Gao, Y. Gao, B. Y. Liu, and Y. Jiang, "Enhanced fault detection and exclusion based on Kalman filter with colored measurement noise and application to RTK," *GPS Solutions*, vol. 25, no. 3, p. 82, 2021.

[22] C. W. Chen and S. S. Kia, "A Renyi divergence based approach to fault detection and exclusion for tightly coupled GNSS/INS system," in *Proceedings of the 2021 International Technical Meeting of the Institute of Navigation*, pp. 674–687, Manassas, VA, 2021.

[23] J. Liu, D. Li, and Z. Xiong, "Research on an improved residual chi-square fault detection method for federated unscented Kalman filter," *Chinese Journal of Scientific Instrument*, vol. 30, pp. 2568–2573, 2009.

[24] J. Duník and O. Straka, "State estimate consistency monitoring in Gaussian filtering framework," *Signal Processing*, vol. 148, pp. 145–156, 2018.

[25] M. Petovello, *Real-Time Integration of a Tactical-Grade IMU and GPS for High-Accuracy Positioning and Navigation*, University of Calgary (Canada), 2003.

[26] Q. Z. Zhang, S. B. Zhang, Z. P. Liu, and H. F. Bian, "Robust cubature Kalman filter based on SVD and its application to integrated navigation," *Control and Decision*, vol. 29, no. 2, pp. 341–346, 2014.

[27] Q. Z. Zhang, X. L. Meng, S. B. Zhang, and Y. J. Wang, "Singular value decomposition-based robust cubature Kalman filtering for an integrated GPS/SINS navigation system," *Journal of Navigation*, vol. 68, no. 3, pp. 549–562, 2015.

[28] R. Gonzalez, J. Giribet, and H. Patiño, "NaveGo: a simulation framework for low-cost integrated navigation systems," *Control Engineering and Applied Informatics*, vol. 17, pp. 110–120, 2015.